Scientia Iranica C (2016) 23(3), 1080–1088

Sharif University of Technology
Scientia Iranica
Transactions C: Chemistry and Chemical Engineering
www.scientiairanica.com

Experimental and theoretical X-ray charge density study of 1-cycloheptylidene-2-(2,4-dinitrophenyl) hydrazine: A hydrazone derivative

Z. Sharafi*

Department of Chemistry, Marvdasht Branch, Islamic Azad University, Marvdasht, Fars, Iran.

Received 3 May 2015; received in revised form 26 July 2015; accepted 15 September 2015

KEYWORDS
X-ray charge density;
Hansen-Coppens formalism;
QTAIM;
Multipolar model.

Abstract. The experimental charge density of a hydrazone derivative has been determined from low temperature (100 K) single crystal X-ray diffraction data by multipolar Hansen-Coppens formalism refinement and gas phase *ab initio* theoretical calculations. The topology of the electron density within the molecule as well as the intramolecular and intermolecular interactions have been analyzed. The topological properties of electron density determined by the experiment were compared with the theoretical results obtained from Gaussian03 at the B3LYP/6-311++G** level of theory. The covalent nature of the bonds in the molecule has been established by (3, -1) bond critical points associated with relatively large electron densities (1.59 - 3.34 e.Å^{-3}) and highly negative Laplacian values (4.73 - 21.30 e.Å^{-5}). Numerical and analytical procedures were used to derive the charges integrated with each atomic basin. The highest charge magnitude (-0.66 e) was found in N2 and N4 atoms. The crystal packing is stabilized by the weak intermolecular π...π, C-H...O and NO_2(N)...(O)NO_2 interactions, as confirmed by the presence of critical points in the topological analysis.

1. Introduction

Intermolecular interactions, such as hydrogen bonds, have been a topic of great scientific interest because of their important role in biological recognition processes and crystal engineering in solid state chemistry [1]. Many of the synthons studied so far in supramolecular chemistry involve classic hydrogen bonds such as N-H...N, N-H...O, O-H...N, and O-H...O, which provide the requisite robustness to create new solid-state structures [2]. In addition to these relatively strong hydrogen bonds, weak interactions such as C-H...O, C-H...N, π...π, and nitro-nitro (NO_2...NO_2) are also important for the self-assembly in the solid state. Therefore, the study of the nature of these interactions, qualitatively and quantitatively, is of great interest. High-resolution low-temperature X-ray diffraction experiments provide accurate information on the electron distribution within the system under study, allowing the qualitative and quantitative nature of the bonding and the atomic interactions to be determined [3]. Bader's quantum theory of Atoms In Molecules (AIM) is a powerful tool, which characterizes the chemical interactions between atoms on the basis of the topological properties of the electron density, $\rho(r)$, and the associated Laplacian, $\nabla^2\rho(r)$, at bond-critical points (bcps). In organic molecules, covalent bonds are classified as the shared shell based on the large value of $\rho(r)$ and negative value of $\nabla^2\rho(r)$, while van der Waals (vdW) and hydrogen-bonding interactions are classified as closed-shell with small large value of $\rho(r)$ and positive $\nabla^2\rho(r)$ [4]. The electron-density distribution of small molecules in chemical systems and peptides and

*. *Tel.: +98 728 3311150-4; Fax: +98 728-3311172*
E-mail address: zahra_sharafi@yahoo.com

amino acids in biochemical systems carries information, which is important for modeling their interactions. The molecular electrostatic potential and electric moments derived from the charge density help to determine the recognition properties, such as reactivity in a desired molecule in a chemical reaction. Due to the importance of the intermolecular C-H...O, $\pi...\pi$, and nitro-nitro ($NO_2...NO_2$) interactions in crystal engineering [5], we decided to obtain an insight of the nature of the chemical bonds and the important molecular interactions of the title compound by X-ray charge density and compare it to the results obtained from the Quantum Theory of Atoms In Molecules (QTAIM) by AIM2000 program package [6].

2. Methods

Accurate low-temperature high-resolution X-ray diffraction data allows the non-spherical maps and electron-density to be presented in the form of deformation electron-density maps and be experimentally quantified by using a non-spherical model of the atomic electron-density. This model is described as a superposition of pseudo-atoms modelled by the multipolar Hansen-Coppens atom formalism (Eq. (1)) [7], implemented in program package MoPro [8], which is the most accurate model, up to now, as follows:

$$\rho_{\text{atom}}(\mathbf{r}) = \rho_{\text{core}}(\mathbf{r}) + P_{val}\kappa^3\rho_{val}(\kappa\mathbf{r}) + \sum_{l=0,l_{\max}} \kappa'^3 R_{nl}(\kappa'\mathbf{r}) \sum_{|m|\leq 1} P_{lm} y_{lm\pm}(\theta,\phi), \quad (1)$$

where ρ_{core} and ρ_{val} represent the spherical core and valence unitary electron-density, respectively. P_{val} is the valence population parameter. $y_{lm\pm}$ represents multipolar spherical harmonic functions of the order l in real form. R_{nl} is Slater-type radial functions and P_{lm} is the multipolar populations. The coefficients κ and κ' describe the contraction-expansion for the spherical and multipolar valence densities, respectively. The low X-ray scattering power of H atoms is a well-known problem in crystallography. However, as it is evident from structures based on neutron diffraction experiments (where the scattering length of H atom is comparable in magnitude with those of heavier elements such as carbon and oxygen), the use of an isotropic displacement parameter for hydrogen is a very crude approximation and should be corrected. Therefore, the program SHADE [9] web server was used to model an estimation of hydrogen anisotropic displacement parameters, which is based on the analysis of displacement parameters of the non-H frameworks as a rigid body in terms of a TLS (translation-liberation-screw) model by Schomaker and Trueblood method [10]. Therefore, the procedure, based on Simple Hydrogen Anisotropic Displacement Estimator (SHADE), calculated the anisotropic displacement parameters for the hydrogen atoms. A first crystal structure refinement was performed with SHELXTL based on the Independent Atom Model (IAM). Then, the least-squares program MoPro was used to determine the charge density of the title compound, as described in Section 3.2.

3. Experimental section

3.1. Data collection and structure determination

The crystal structure of the title compound was determined by single-crystal X-ray diffraction. The crystallographic data of the compound is listed in Table 1. The ORTEP plot of the compound is shown in Figure 1, with 50% probability displacement ellipsoids and atomic numbering. Data was collected on a Bruker SMART APEX II CCD area detector diffractometer with Mo $K\alpha$ radiation (λ = 0.71073Å) equipped with an Oxford cryo-system Cobra low temperature attachment. Cell parameters were retrieved using SMART [11] software and refined using SAINT [12] on all observed reflections. Data reduction and correction for Lorentz-polarization (Lp) and decay were performed using SAINT Plus software. Absorption corrections were applied using SADABS [13]. The structure was solved by direct methods and refined by the least squares method on F^2 using the SHELXTL program package [14]. All non-hydrogen atoms were refined anisotropically. Hydrogen atoms were positioned geometrically and refined with a riding model approximation with their parameters constrained to the parent atom with U_{iso} (H) = 1.2 U_{eq} (C), except for the hydrogen atom attached to N1 atom which was located by the difference Fourier map and constrained to be refined with the parent atom with U_{iso} (H) = 1.2 U_{eq} (N).

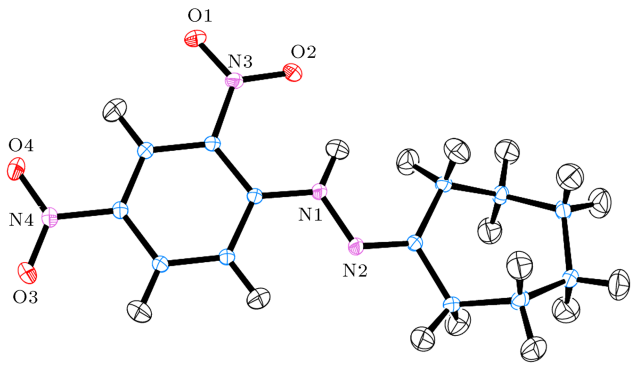

Figure 1. The ORTEP plot of the title compound based on the multipolar refinement with 50% probability displacement ellipsoids. The anisotropic displacement ellipsoids of the hydrogen atoms were calculated by SHADE program.

Table 1. The crystallographic data and refinement parameters of the compound by IAM.

Empirical formula	$C_{13}H_{16}N_4O_4$
Formula weight	222.30
Temperature	100(1) K
Crystal system	Monoclinic
Space group	$P2_1/n$
a (Å)	6.9721(1)
b (Å)	23.7359(5)
c (Å)	8.2274(2)
β (Å)	102.351(1)
V(Å^3)	1330.03(5)
Z	4
D (Mg/m^3)	1.460
μ (mm^{-1})	0.111
Crystal size (mm)	0.96 × 0.61 × 0.08
Max. and min. θ	1.7, 35.0
Limiting indices	$-11 \leq h \leq 11$, $-38 \leq k \leq 38$, $-12 \leq l \leq 13$
Reflections collected/unique	26146 / 5824 [R(int) = 0.026]
Data/restraints/parameters	5824/0/194
GoF	1.04
Final R indices [$I > 2\sigma(I)$]	R1 = 0.0388, wR2 = 0.1132
Largest diff. peak and hole	0.43 and -0.30 e.Å^{-3}

3.2. Multipolar model refinement

Initially, an Independent Atom Model (IAM) approximation with routine least-square refinement model was used for refining the structure. The parameters refined in the successive steps of multipolar model refinement were as follow: (i) the scale factor with all reflections; (ii) the atomic fractional coordinates together with Anisotropic Displacement Parameters (ADP) for non-hydrogen atoms with high angle diffraction data (sin $\theta/\lambda > 0.8$ Å^{-1}); (iii) the positional coordinates and isotropic displacement parameters of H-atoms using low-angle diffraction data (sin $\theta/\lambda < 0.8$ Å^{-1}); (iv) the hydrogen atom positions (the N-H and C-H bonds elongated to distances 1.03 Å and 1.09 Å, respectively, resulted from the neutron diffraction data) and the displacement parameters of non-hydrogen atoms at high-angle diffraction data (sin $\theta/\lambda > 0.8$ Å^{-1}); (v) estimation of anisotropic displacement parameters for H atoms using the SHADE2 program; (vi) multipole parameters refinement in a stepwise procedure; (vii) atomic fractional coordinates and displacement parameters along with all multipole populations; and (viii) atomic fractional coordinates as well as displacement parameters together with all multipole populations and κ and κ' (only non-H atoms) parameters.

3.3. DFT and AIM calculations

The starting atomic coordinates were taken from the final X-ray refinement cycle of the structure analysis. For the ground state electronic structure calculations, the DFT method with the Becke [15] three-parameter hybrid functional and Lee-Yang-Parr's [16] gradient corrected correlation functional (B3LYP) was used for full optimization of the single molecule and the hydrogen bonded dimers in gas phase. The calculations were performed with the Gaussian03 (G03) [17] program with 6-311++G** basis set for all atoms. Then, the obtained ground-state electronic wave functions were used for further calculations on the topology of the theoretical electron density, including both local and integral properties, performed with the aid of the program AIM2000.

4. Results and discussion

It is well known that the quantum theory of atoms in molecules (QTAIM) provides a powerful tool for char-

acterization of the nature of the chemical bonds [18]. It uses the electron density as an information source to describe atoms and the nature of the bonds in molecules. In QTAIM, a chemical bond (including covalent, ionic, van der Waals and hydrogen bonds, etc.) is always accompanied with a Bond Path (BP) and a Bond Critical Point (BCP) between the bonded atoms. Therefore, shared-shell interactions, such as covalent bonds, are characterized by the significant positive values of the electron density and negative values of the Laplacian of the electron density at the bond critical points (bcps). On the other hand, the closed-shell interactions, such as ionic bonding, van der Waals (vdW) and hydrogen bonding, tend to have small positive values for both electron density and its Laplacian at the bond critical points (bcps). The molecular graphs (the set of BPs and BCPs) of the single molecules of this work have been shown in Figure 2. As indicated, in addition to the usual bonds, the molecular graphs indicate a BP and a BCP between nitrogen and hydrogen, which confirms that there is an intramolecular hydrogen bond in the molecule. The topological properties at the critical points identified for the compound are listed in Table 2. The deformation density map of the benzene

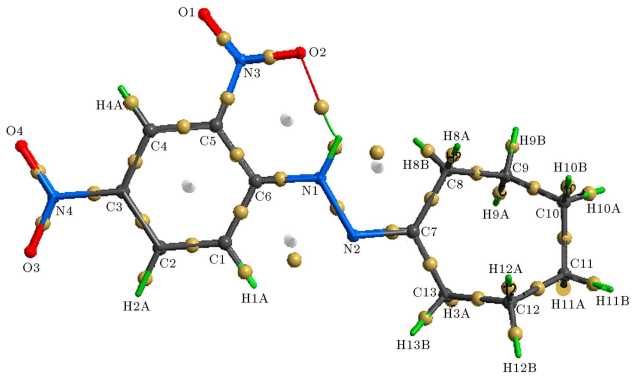

Figure 2. The molecular graph of the molecule showing critical points and the bond path.

Table 2. Topological properties of the title compound at the bond critical points (bcps). The theoretical values of $\rho(r)$ and $\nabla^2\rho(r)$ are shown bold in parentheses.

Bond	$\rho(r)$ e.Å^{-3} [in a.u.]	$\nabla^2\rho(r)$ e.Å^{-5} [in a.u.]	ε	Type
O1-N3	3.254 [0.48] **(0.49)**	-8.60 [-0.36] **(-1.00)**	0.12	(3,-1)
O2-N3	3.094 [0.46] **(0.47)**	-15.14 [-0.22] **(-0.88)**	0.11	(3,-1)
O2...H1N1	0.165 [0.02] **(0.03)**	2.95 [0.12] **(0.12)**	0.26	(3,-1)
O3-N4	3.300 [0.49] **(0.48)**	-9.62 [-0.40] **(-0.48)**	0.09	(3,-1)
O4-N4	3.342 [0.49] **(0.49)**	-6.61 [-0.27] **(-1.00)**	0.13	(3,-1)
N1-N2	2.199 [0.32] **(0.33)**	-4.73 [-0.20] **(-0.28)**	0.07	(3,-1)
N1-C6	2.137 [0.32] **(0.32)**	-21.30 [-0.88] **(-0.88)**	0.13	(3,-1)
N1-H1N1	2.142 [0.32] **(0.46)**	-27.53 [-1.14] **(-3.40)**	0.08	(3,-1)
N2-C7	2.414 [0.36] **(0.36)**	-20.74 [-0.86] **(-0.76)**	0.16	(3,-1)
N3-C5	1.824 [0.27] **(0.27)**	-14.54 [-0.60] **(-0.68)**	0.23	(3,-1)
N4-C3	1.793 [0.26] **(0.28)**	-12.91 [-0.54] **(-0.68)**	0.19	(3,-1)
C1-C2	2.179 [0.32] **(0.32)**	-21.30 [-0.88] **(-0.88)**	0.21	(3,-1)
C1-C6	1.966 [0.29] **(0.29)**	-16.83 [-0.70] **(-0.76)**	0.20	(3,-1)
C2-C3	2.053 [0.30] **(0.30)**	-18.55 [-0.77] **(-0.84)**	0.21	(3,-1)
C3-C4	2.202 [0.33] **(0.32)**	-20.74 [-0.86] **(-0.88)**	0.26	(3,-1)
C4-C5	2.135 [0.32] **(0.31)**	-20.02 [-0.84] **(-0.84)**	0.26	(3,-1)
C5-C6	1.966 [0.29] **(0.29)**	-17.10 [-0.71] **(-0.76)**	0.23	(3,-1)
C7-C8	1.686 [0.25] **(0.25)**	-11.31 [-0.47] **(-0.56)**	0.10	(3,-1)
C7-C13	1.698 [0.25] **(0.25)**	-11.79 [-0.49] **(-0.60)**	0.04	(3,-1)
C8-C9	1.595 [0.24] **(0.24)**	-8.99 [-0.37] **(-0.48)**	0.06	(3,-1)
C9-C10	1.625 [0.24] **(0.24)**	-9.68 [-0.40] **(-0.52)**	0.06	(3,-1)
C10-C11	1.644 [0.24] **(0.24)**	-9.68 [-0.40] **(-0.52)**	0.05	(3,-1)
C11-C12	1.643 [0.24] **(0.24)**	-9.18 [-0.38] **(-0.52)**	0.07	(3,-1)
C12-C13	1.584 [0.23] **(0.23)**	-8.56 [-0.36] **(-0.48)**	0.04	(3,-1)
N3...O3	0.043 [0.006] **(0.007)**	0.73 [0.03] **(0.028)**	1.97	(3,-1)
C2...C6	0.037 [0.006] **(0.006)**	0.39 [0.016] **(0.0158)**	1.16	(3,-1)
O3...H2A	0.047 [0.007] **(0.007)**	0.91 [0.038] **(0.027)**	0.27	(3,-1)

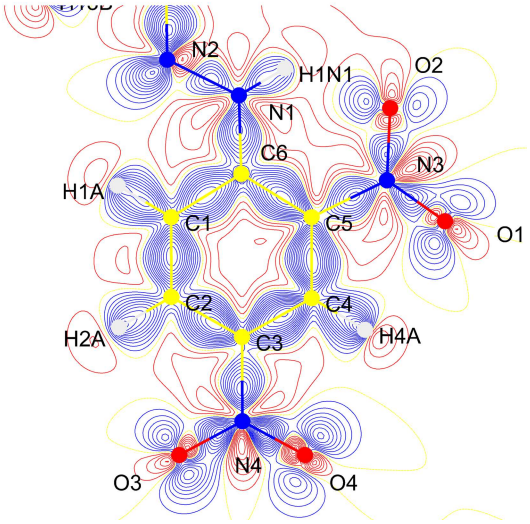

Figure 3. Experimental deformation density maps in the plane of the benzene ring (contours at 0.1 e Å^{-3}, blue/red: positive/negative).

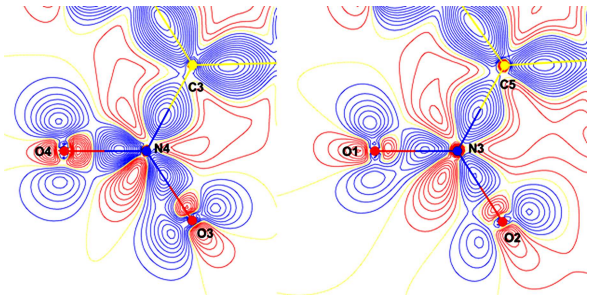

Figure 4. Experimental deformation density maps in the plane of the benzene ring (contours at 0.1 e Å^{-3}, blue/red: positive/negative).

ring and both nitro groups are shown in Figures 3 and 4, respectively. The Laplacian of the electron density for benzene ring and both nitro groups are also shown in Figures 5 and 6. Each of the carbon-carbon, carbon-nitrogen, and nitrogen-oxygen bonds having shared-shell covalent interactions based on the quantity of the electron density and Laplacian are listed in Table 2. The average electron density of the C-C bonds of the benzene ring is close to 2.1 e Å^{-3}, which is consistent with the value for the aromatic ring [19]. The values of the electron density and the Laplacian for C6-N1 bond are higher than those for C3-N4 and C5-N3, which is in agreement with the nature of the bond and the atoms attached to each other. The average $\nabla^2\rho(r)$ value of the C-C bonds in the benzene ring [-19.09 e Å^{-5}] is in agreement with that in a delocalized aromatic ring. An analysis for bond-path has been performed to determine the nature of the bond polarization. The lower values of the Laplacian for the nitro groups confirm low concentration of the electron density compared to the aromatic ring. The high negative value of the Laplacian

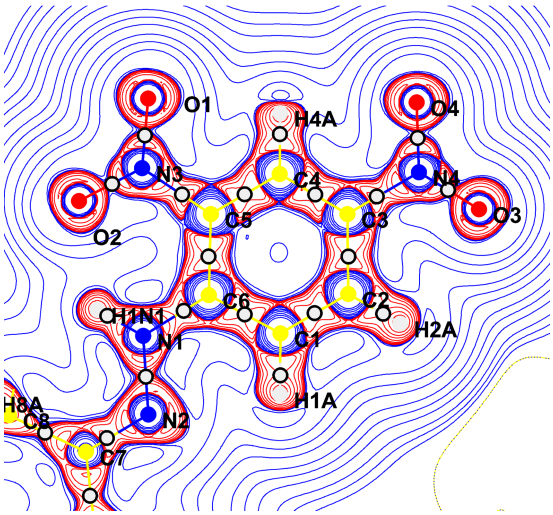

Figure 5. Laplacian of the electron density for the title compound; positive contours are dashed red lines, negative contours are dashed blue lines.

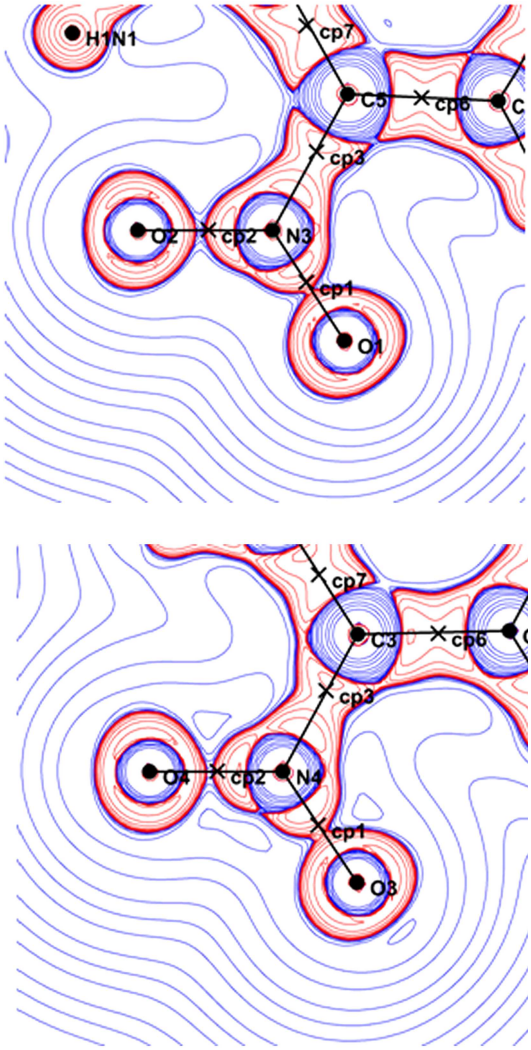

Figure 6. Laplacian of the electron density in the plane of nitro groups; positive contours are dashed red lines, negative contours are dashed blue lines.

[-27.53 e Å^{-5}] for N1-H1N1 bond confirms the high concentration of the bond electron density. The nitro N-O bond critical points have the smallest negative Laplacian values, which is mostly due to the principal curvature along the bonds (average λ_3 value for all N-O bonds = 49.03 eÅ^{-5}) and is in agreement with the previously reported nitro-substituted compounds [20]. The experimental values of the electron density and its Laplacian are in good agreement with their theoretical values for single molecule and the dimers obtained by the wave function calculations by AIM2000. The differences between the experimental and theoretical values of $\nabla^2\rho(r)$ in some cases are related to the deficiency of the multipole model description of the electron density [21,22]. The experimental properties of the strongly polarized bond are different from the results derived by ab initio calculations. The results show that the descriptions of the polar bonds require more flexible basis sets in the theoretical calculations. The bond ellipticity ($\varepsilon = \lambda_1/\lambda_2 - 1$) is a measure of isotropic or anisotropic nature of the bonds, where λ_1 and λ_2 are the negative eigenvalues of the Hessian matrix [23]. The calculated ellipticities for all bonds show that the C-C and C-N bonds in the benzene ring and the iminic N=C bond have anisotropic nature as their ellipticity is close to 0.2. The interesting features of the packing are the intermolecular C2-H2A...O3 hydrogen bond and (NO_2)N3...O3(NO_2) interaction. The Laplacian of the electron density maps of these interactions are shown in Figures 7 and 8, respectively, and their electron density and Laplacian values are listed in Table 2, which confirm the shared-shell nature of these interactions. Figure 9 shows the Laplacian of the electron density of the intermolecular $\pi...\pi$ interactions. Figure 10 shows the gradient trajectory plot of the electron density, $\rho(r)$, plotted using WinXPRO software [24]. In the plot, the solid thick lines show the zero-flux surface of the atoms in the molecule and define the boundary of the atomic basin for each atom. O1, O2, O3, O4, N1, and N2 basins show large volumes compared with the other atoms in the molecule. The volume of the carbon atom looks prismatic, whereas the oxygen atom is in a drop shape. The gradient trajectory lines are dominant in the core of the atomic basin and decrease away from the nucleus. The atomic volume of the O1 atom is 15.70 Å^3 and the atomic volume of the N atoms ranges from 6.93 to 13.91 Å^3, so the atomic volume of the O1 is much higher than those of the

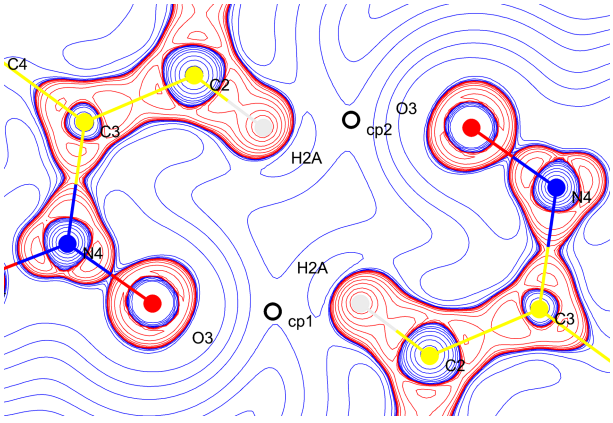

Figure 7. Laplacian of the electron density in the plane of the symmetry-related intermolecular C-H...O interactions; positive contours are red lines, negative contours are blue lines.

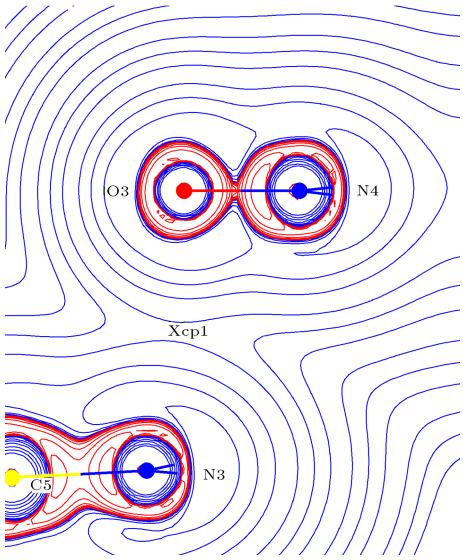

Figure 8. Laplacian of the electron density of the interaction between (NO_2)O...N(NO_2) in the neighboring nitro groups; positive contours are dashed red lines, negative contours are dashed blue lines (the cross shows the critical point).

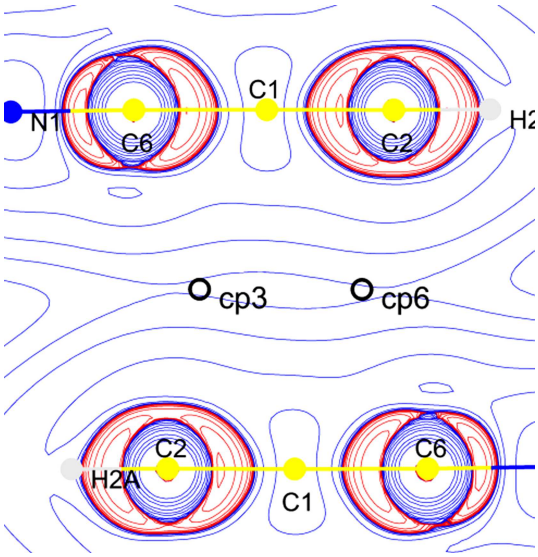

Figure 9. Laplacian of the electron density of the interaction between C2...C6 in the neighboring benzene rings (the circle shows the critical point).

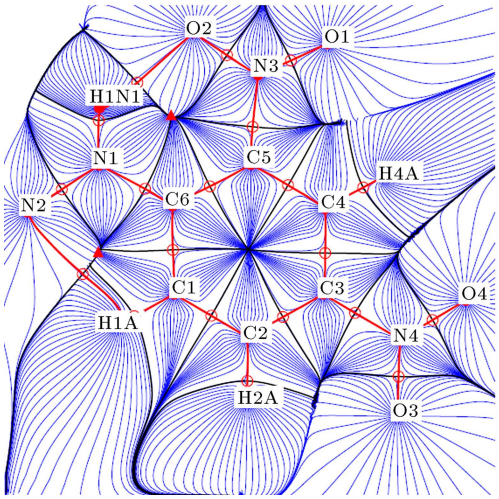

Figure 10. Representation of the trajectory of the gradient lines of the total electron density in the plane of the substituted benzene ring.

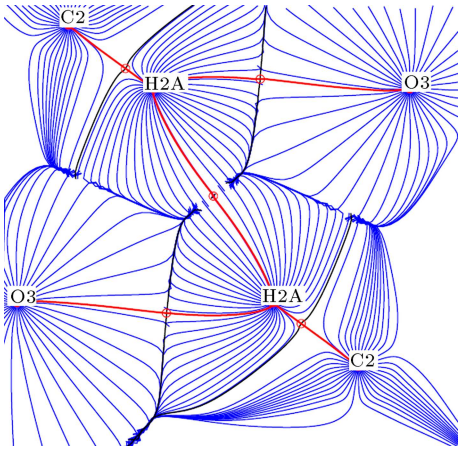

Figure 11. Representation of the trajectory of the gradient lines of the total electron density of the centerosymmetric intermolecular C2-H2A...O3 interactions.

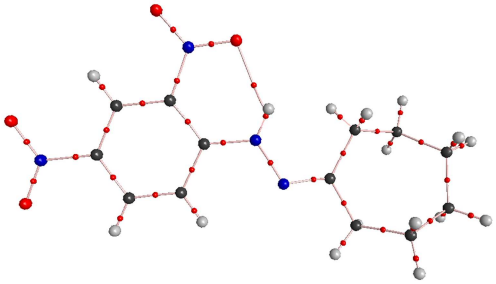

Figure 12. The molecular graph of the molecule showing the position of the bond critical points (red circles).

rest of the other non-oxygen atoms in the molecule. The atomic values of H2A and H1N1 atoms have the smallest value in the molecule, confirming that they are involved in hydrogen bonding interactions. Generally, the atoms which are involved in the hydrogen bonding interaction have smaller atomic volume than

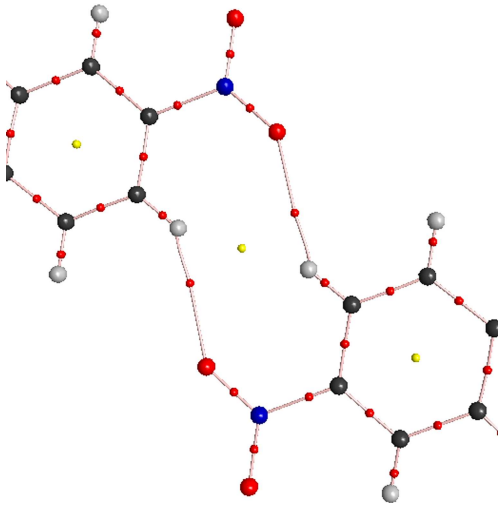

Figure 13. A part of the molecular graph of the compound showing intermolecular centerosymmetric C-H...O interactions with the position of the bond critical points (red circles).

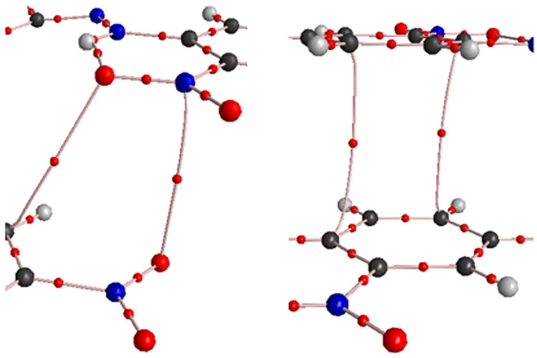

Figure 14. A part of the molecular graph of the compound showing $(NO_2)N...O(NO_2)$ (left) and $\pi...\pi$ interactions (right) with the position of the bond critical points (red circles).

the other atoms which are not involved in hydrogen-bonding interactions [25]. The details of the gradient trajectory plots of the intermolecular hydrogen-bonding C2-H2A...O3 are shown in Figure 11. As can be seen from the values of the electron density and the Laplacian, the C2-H2A...O3 and N1-H1N1...O2 interactions are closed-shell interactions. For pursuing the agreement between the experimental and theoretical charge densities, the theoretical calculations were done for the single molecule and also dimer with different interactions, such as intermolecular C-H...O, $(NO_2)N...O(NO_2)$, and $\pi...\pi$ by AIM package. Figure 12 shows the molecular graph of the single molecule calculated by AIM2000 with the position of the bond critical points as red circles. Figure 13 shows the molecular graph of a centerosymmetric dimer connected by the intermolecular C-H...O interactions. Figure 14 depicts the molecular graphs of the compound based on the N...O interaction of the

Table 3. Atomic charges (e) and volumes (Å3) of the compound.

Atoms	$q(P_v)$	Volume
O1	-0.42	15.70
O2	-0.18	15.73
O3	-0.40	16.02
O4	-0.53	15.88
N1	-0.54	12.46
N2	-0.66	13.90
N3	-0.45	6.93
N4	-0.66	7.47
C1	-0.05	12.46
H1A	+0.20	5.96
C2	+0.17	11.13
H2A	+0.18	5.87
C3	+0.25	9.27
C4	-0.12	11.88
H4A	+0.18	5.68
C5	+0.29	9.80
C6	+0.73	7.49
C7	+0.64	7.25
C8	+0.20	7.79
H8A	0.00	7.14
H8B	+0.16	6.43
C9	-0.02	8.30
H9A	-0.08	7.25
H9B	0.00	6.39
C10	-0.22	8.70
H10A	-0.08	7.95
H10B	-0.09	7.61
C11	-0.10	8.30
H11A	-0.19	7.22
H11B	-0.16	9.41
C12	+0.01	7.98
H12A	-0.11	7.67
H12B	-0.09	7.80
C13	-0.09	8.63
H13A	+0.01	6.40
H13B	-0.08	7.37
H1N1	+0.58	2.22

neighboring nitro groups and the intermolecular $\pi...\pi$ interaction, which confirms the experimental results obtained by the high-resolution X-ray charge density in this study. The atomic charges and volumes of each atom were calculated. The atomic charges can be defined as the difference between the nuclear and electronic charges integrated over the atomic basins by zero-flux surfaces [4]. The net monopole charges of each atom in the compound were calculated using WinXPRO for the experimental model. The O1, O2, O3, O4, N1, N2, and N4 atoms carry high negative charges of -0.42e, -0.18e, -0.40e, -0.53e, -0.54e, -0.66e and -0.66e, respectively. The details of the atomic charges and volumes for each atom are shown in Table 3.

5. Conclusion

The current study provides an extensive charge density study of a hydrazone derivative crystal using high-resolution X-ray experimental data collection at 100 K. The theoretical wave function calculations using Gaussian03 were used to model the theoretical charge density of the compound by B3LYP level of theory and 6-311++G** basis set with diffuse functions. The topological properties of critical points have been analyzed using Bader's theory of Atoms In Molecules (AIM) for the quantification of covalent bonds and intermolecular interactions. The results obtained from the topological analysis of the multipole modeled densities agree quite well to the theoretical calculations, but the largest discrepancies being found for the Laplacian at the bond critical point of strong heteroatom bonds.

Acknowledgment

The author thanks the Islamic Azad University of Marvdasht for the support of this work.

References

1. Desiraju, G.R., *Crystal Engineering: The Design of Organic Solids*, Elsevier, New York (1989).
2. Allen, F.H., Motherwell, W.D.S., Raithby, P.R., Shields, G.P. and Taylor, R. "Systematic analysis of the probabilities of formation of bimolecular hydrogen-bonded ring motifs in organic crystal structures", *New J. Chem.*, **23**, pp. 25-34 (1999).
3. Scheins, S., Messerschmidt, M. and Luger, P. "Submolecular partitioning of morphine hydrate based on its experimental charge density at 25 K", *Acta Cryst.*, **B61**, pp. 443-448 (2005).
4. Bader, R.F.W., *Atoms in Molecules, A Quantum Theory*, Oxford University Press (1990).
5. Daszkiewicz, M. "Importance of O...N interaction between nitro groups in crystals", *Cryst. Eng. Com.*, **15**, pp. 10427-10430 (2013).
6. Biegler-König, F. and Schönbohm, J. "Update of the AIM2000-program for atoms in molecules", *J. Comput. Chem.*, **23**(15), pp. 1489-1494 (2002).
7. Hansen, N.K. and Coppens, P. "Testing aspherical atom refinements on small-molecule data sets", *Acta Cryst.*, **A34**, pp. 909-921 (1978).
8. Zarychta, B., Pichon-Pesme, V., Guillot, B., Lecomte, C. and Jelsch, C. "On the application of an experimental multipolar pseudo-atom library for accurate refinement of small-molecule and protein crystal structures", *Acta Cryst.*, **A38**, pp. 38-54 (2006).
9. Madsen ϕstergaard, A. "SHADE web server for estimation of hydrogen anisotropic displacement parameters", *J. Appl. Cryst.*, **39**, pp. 757-758 (2006).

10. Schomaker, V. and Trueblood, K.N. "On the rigid-body motion of molecules in crystals", *Acta Cryst.*, **B24**, pp. 63-76 (1968).
11. *SMART: Bruker Molecular Analysis Research Tool*, Bruker AXS Inc., Madison, Wisconsin, USA (2005).
12. SAINT (Version V7.12A), *Data Reduction and Correction Program,* Bruker AXS Inc., Madison, Wisconsin, USA (2005).
13. SADABS (Version 2004/1), *An Empirical Absorption Correction Program*, Bruker AXS Inc., Madison, Wisconsin, USA.
14. Sheldrick, G.M. "A history of SHELXL", *Acta Cryst.*, **A64**, pp. 112-122 (2008).
15. Becke, A.D. "Density-functional thermochemistry. III. The role of exact exchange", *J. Chem. Phys.*, **98**, pp. 5648-5652 (1993).
16. Lee, C., Yang, W. and Parr, R.G. "Development of the Colle-Salvetti correlation-energy formula into a functional of the electron density", *Phys. Rev. B: Condens Matter*, **37**, pp. 785-789 (1998).
17. Frisch, M.J. et al., *Gaussian 03*, Revision B.04; Gaussian, Inc.: Wallingford, CT (2004).
18. Popelier, P.L.A., *Atoms in Molecules; An Introduction*, Prentice Hall, UK (2000).
19. Hibbs, D.E., Hanrahan, J.R., Hursthouse, M.B., Knight, D.W., Overgaard, J., Turner, P., Piltz, R.O. and Waller, M.P. "X-N charge density analysis of hydrogen bonding motifs in 1-(2-hydroxy-5-nitrophenyl)ethanone", *Org. Biomol. Chem.*, **1**, pp. 1034-1040 (2003).
20. Kubicki, M., Borowiak, T., Dutkiewicz, G., Souhassou, M., Jelsch, C. and Lecomte, C. "Experimental electron density of 1-phenyl-4-nitroimidazole and topological analysis of C-H...O and C-H...N hydrogen bonds", *J. Phys. Chem. B*, **106**, pp. 3706-3714 (2002).
21. Messerschmidt, M., Wagner, A., Wong, M.W. and Luger, P. "X-ray charge density study of N_2O_4", *J. Am. Chem. Soc.*, **124**, pp. 732-733 (2002).
22. Tsirelson, V.G., Stash, A.I., Potemkin, V.A., Rykounov, A.A., Shutalev, A.D., Zhurova, E.A., Zhurov, V.V., Pinkerton, A.A., Gurskaya, G.V. and Zavodnik, V.E. "Molecular and crystal properties of ethyl 4,6-dimethyl-2-thioxo-1,2,3,4-tetrahy- dropyrimidine-5 -carboxylate from experimental and theoretical electron densities", *Acta Cryst.*, **B62**, pp. 676-688 (2006).
23. Cramer, D. and Kraka, E. "A description of the chemical-bond in terms of local properties of electron-density and energy", *Croat. Chem. Acta*, **57**, pp. 1259-1281 (1984).
24. Stash, A.I. and Tsirelson, V.G. "Developing WinXPRO: a software for determination of the multipole-model-based properties of crystals", *J. Appl. Cryst.*, **47**, pp. 2086-2089 (2014).
25. Koch, U. and Popelier, P.L.A. "Characterization of CHO hydrogen bonds on the basis of the charge density", *J. Phys. Chem.*, **99**, pp. 9747-9754 (1995).

Biography

Zahra Sharafi was born in Shiraz, Iran. She received her BSc, MSc, and PhD degree from Shiraz University under supervision of Professor Ali Boushehri. She is currently Assistant Professor of Physical Chemistry. Her research interests include thermodynamic study of chemical systems and also X-ray charge denisty of small organic compounds.